

General Disclaimer

One or more of the Following Statements may affect this Document

- This document has been reproduced from the best copy furnished by the organizational source. It is being released in the interest of making available as much information as possible.
- This document may contain data, which exceeds the sheet parameters. It was furnished in this condition by the organizational source and is the best copy available.
- This document may contain tone-on-tone or color graphs, charts and/or pictures, which have been reproduced in black and white.
- This document is paginated as submitted by the original source.
- Portions of this document are not fully legible due to the historical nature of some of the material. However, it is the best reproduction available from the original submission.

(NASA-TM-83973) HOLOGRAMS FOR LASER DIODE:
SINGLE MODE OPTICAL FIBER COUPLING (NASA)
48 p HC A03/MF A01

CSCL 14E

N83-19073

Unclassified
G3/35 08900



Technical Memorandum 83973

Holograms for Laser Diode - Single Mode Optical Fiber Coupling

Peter L. Fuhr

APRIL 1982

National Aeronautics and
Space Administration

Goddard Space Flight Center
Greenbelt, Maryland 20771



HOLOGRAMS FOR LASER DIODE - SINGLE MODE OPTICAL FIBER COUPLING

Peter L. Fuhr
NASA/Goddard Space Flight Center
Greenbelt, Maryland 20771

ABSTRACT

The low coupling efficiency of semiconductor laser emissions into single mode optical fibers place a severe restriction on their use. Associated with these conventional optical coupling techniques are stringent alignment sensitivities. Using holographic elements, the coupling efficiency may be increased and the alignment sensitivity greatly reduced. Both conventional and computer methods used in the generation of the holographic couplers are described and diagrammed. The reconstruction geometries used are shown to be somewhat restrictive but substantially less rigid than their conventional optical counter-parts. Single and double hologram techniques are examined concerning their respective ease of fabrication and relative merits.

CONTENTS

	<u>Page</u>
ABSTRACT.....	i
TABLE OF CONTENTS.....	ii
TABLE OF FIGURES.....	iii
I. INTRODUCTION.....	1
II. WAVEFRONT CONVERSION COUPLER.....	3
III. COUPLING EFFICIENCY.....	8
IV. DOUBLE HOLOGRAM TECHNIQUE.....	11
V. TWO-BEAM HOLOGRAPHIC FABRICATION.....	13
VI. COMPUTER GENERATED HOLOGRAMS.....	13
A. Introduction.....	13
B. Fourier Transform Holograms.....	20
C. Experiment - A Computer Generated Binary Fourier Transform Hologram.....	22
VII. CONCLUSIONS.....	29

FIGURES

	<u>Page</u>
Figure 1.....	6
Figure 2.....	9
Figure 3.....	10
Figure 4.....	12
Figure 5a.....	14
Figure 5b.....	15
Figure 6.....	16
Figure 7.....	19
Figure 8.....	21
Figure 9.....	23
Figure 10.....	25
Figure 11.....	27
Figure 12.....	28

ILLUSTRATIONS

1. CGHBLACKP.FOR Program Listing.....	31
2. PF.FOR Computer Listing.....	36

REFERENCES.....	43
-----------------	----

HOLOGRAMS FOR LASER DIODE - SINGLE MODE OPTICAL FIBER COUPLING

I. INTRODUCTION

The use of optical fibers for the propagation of light emitted from a semiconductor laser (or laser diode, LD) has been an area of intense study for the past 5-10 years. Single mode LDs, in which only the fundamental mode is emitted, are proving to be a most attractive source for high data rate optical communication systems. When the output from a single mode LD is coupled into a single mode optical fiber, fiber dispersion (the spreading of the pulse shape due to differing propagation speeds for the modes in the fiber) is eliminated. Another benefit in using single mode optical fibers is that the emerging beam is well-behaved spatially, having a Airy disk far-field diffraction pattern.

In the past five years, a great deal of effort has been expended in decreasing the fiber transmission losses. With these losses now on the order of 0.2 dB per kilometer, emphasis has been turned to the large losses associated with coupling the LD output into the fiber (1-4).

The techniques currently employed for the coupling of LD light into a fiber consist of the following:

1. Butt-end joint: The fiber is cleaved so that its front face is perpendicular to the fiber core. It is then butted up against the LD.

2. **Tapered fiber:** Some of the fiber's cladding is etched off, by chemical or mechanical means, exposing the fiber's core. It is then positioned near the front facet on the LD.
3. **Fiber-tip microlens:** The tip of the fiber is melted and formed into a hemispherical lens. This end is then positioned such that the LD is at the lens' focal point.
4. **Conventional optics:** Lenses (typically 2 crossed cylindrical lenses) are placed in front of the LD to conform its output beam and focus it onto the fiber's core.

These techniques provide coupling efficiencies of less than 40%*. (The 40% figure has been reported in technical journal articles a laboratory results. A reproducible coupling efficiency of 20% is considered quite good (5)). The causes of this poor coupling efficiency are primarily attributable to the small acceptance angle of the fiber's 5 micron core (Numerical Aperture of about 0.2), and the large non-symmetric divergence of the LD beam (20 and 80 degrees parallel and perpendicular to the 0.7 micron by 10 micron LD lasing region. All of these techniques also result in very stringent alignment tolerances for the positioning of the fiber and any other optical elements, with respect to the LD front facet. Alignments of approximately 1-2 microns perpendicular and parallel to the LD front facet must be maintained for losses

*The coupling efficiency is given by the ratio of the amount of power launched into the fiber and the LD's output power.

of less than 1 dB. The spacing between the LD and fiber directly impacts coupling. The alignment tolerances in this case are in the 20 micron range for <1 dB loss.

II. WAVEFRONT CONVERSION COUPLER

A different approach to this problem is to examine the wavefronts of LD and fiber in the Fraunhofer diffraction region. At some plane in between the two devices these fields can be superimposed resulting in an interference pattern. Theoretically, if some sort of wavefront converting structure could be constructed and placed in this plane to effectively match the two "antennas" (the LD and the fiber), a coupling efficiency of 100% could result. This procedure would actually convert the wavefront diverging from the LD into the Airy disk far-field pattern of the fiber. This type of wavefront conversion falls into the general category of holography. So if a hologram representing the wavefront converting structure would be placed in this plane and then illuminated by the LD emission used to construct the hologram, all of the LD light impinging on the hologram would have its wavefront changed into the fiber's Fraunhofer diffraction pattern. The converted wavefront would then be totally accepted by the fiber core.

In considering diffraction from an aperture, the Fraunhofer region is defined as the distance, Z , from the aperture where the phase change over the aperture is assumed to be much less than 1 radian. If the aperture is considered to be rectangular with the maximum value of $x_1^2 + y_1^2 = (d/2)^2$ where d is the linear dimension of the maximum extent of the aperture, then this phase restriction implies:

ORIGINAL PAGE IS
OF POOR QUALITY

$$K \frac{(x_1^2 + y_1^2)^{\max}}{2z} = K \frac{(d/2)^2}{2z} = \frac{\pi d^2}{4\lambda z} \ll 1 \quad (1)$$

$$\text{or } z \gg d^2 / \lambda \quad (2)$$

Single-mode optical fibers have core diameters of 4-8 microns. LDs' maximum front-facet linear dimension is typically 10 microns. For the fiber and LD, the Fraunhofer assumption implies, assuming light with wavelength 830 nanometers.

$$z_f \gg \frac{d_f^2}{\lambda} = 77 \text{ microns}$$

$$z_{LD} \gg \frac{d_{LD}^2}{\lambda} = 120 \text{ microns}$$

Thus, if the hologram's positioning plane is chosen to be 150 microns away from the LD and fiber, the Fraunhofer diffraction condition is valid.

The amplitude distribution in the Fraunhofer diffraction pattern of the circular fiber core is the Airy disk pattern given by:

$$U(r_o) = \exp(jkz) \exp\left(j \frac{K r_o^2}{2z}\right) \left(\frac{K l}{j8z}\right) \left[\frac{2J_1\left(\frac{K l r_o}{2z}\right)}{\left(\frac{K l r_o}{2z}\right)} \right] \quad (3)$$

where l is the radius of the fiber core; r is the radius coordinate in the observation plane; z is the distance from the aperture (fiber core) to the observation plane; and J_1 is the first order Bessel function.

ORIGINAL PAGE IS
OF POOR QUALITY

$$\text{With: } r_o^2 = x_o^2 + y_o^2$$

$$U(x_o, y_o) = \exp(jKz) \exp\left(j \frac{K(x_o^2 + y_o^2)}{2z}\right) \left(\frac{Kl}{j8z}\right)^2 \left[2J_1\left(\frac{Kl\sqrt{x_o^2 + y_o^2}}{2z}\right) \right]$$

$$= A(x_o, y_o) \exp(j\phi(x_o, y_o)) \quad (4)$$

Similarly, the electric field a distance Z away from the LD's front facet is given by the Fraunhofer diffraction pattern for a rectangular aperture.*

$$U(x_o, y_o) = \exp(jKz) \exp\left(j \frac{K(x_o^2 + y_o^2)}{2z}\right) l_x l_y \text{sinc}\left(\frac{l_x x_o}{\lambda z}\right) \text{sinc}\left(\frac{l_y y_o}{\lambda z}\right)$$

$$= a(x_o, y_o) \exp(j\Psi(x_o, y_o)) \quad (5)$$

where l_x is the linear dimension of the aperture in the x direction; l_y is the linear dimension in the y direction.

With the elements positioned as in Figure 1, the electric field at the plane P is given by the superposition of the two incident fields U_{LD} and U_f .

$$U_p = U_{LD} + U_f$$

The resultant intensity distribution is: $I_p = |U_p U_p^*|$

*Equations (3) through (5) were derived assuming plane waves incident on the aperture. The field incident on the front facet of the single-mode LD (TE_{10} mode) is roughly planar, as in the case for a rectangular waveguide (6).

ORIGINAL PAGE IS
OF POOR QUALITY

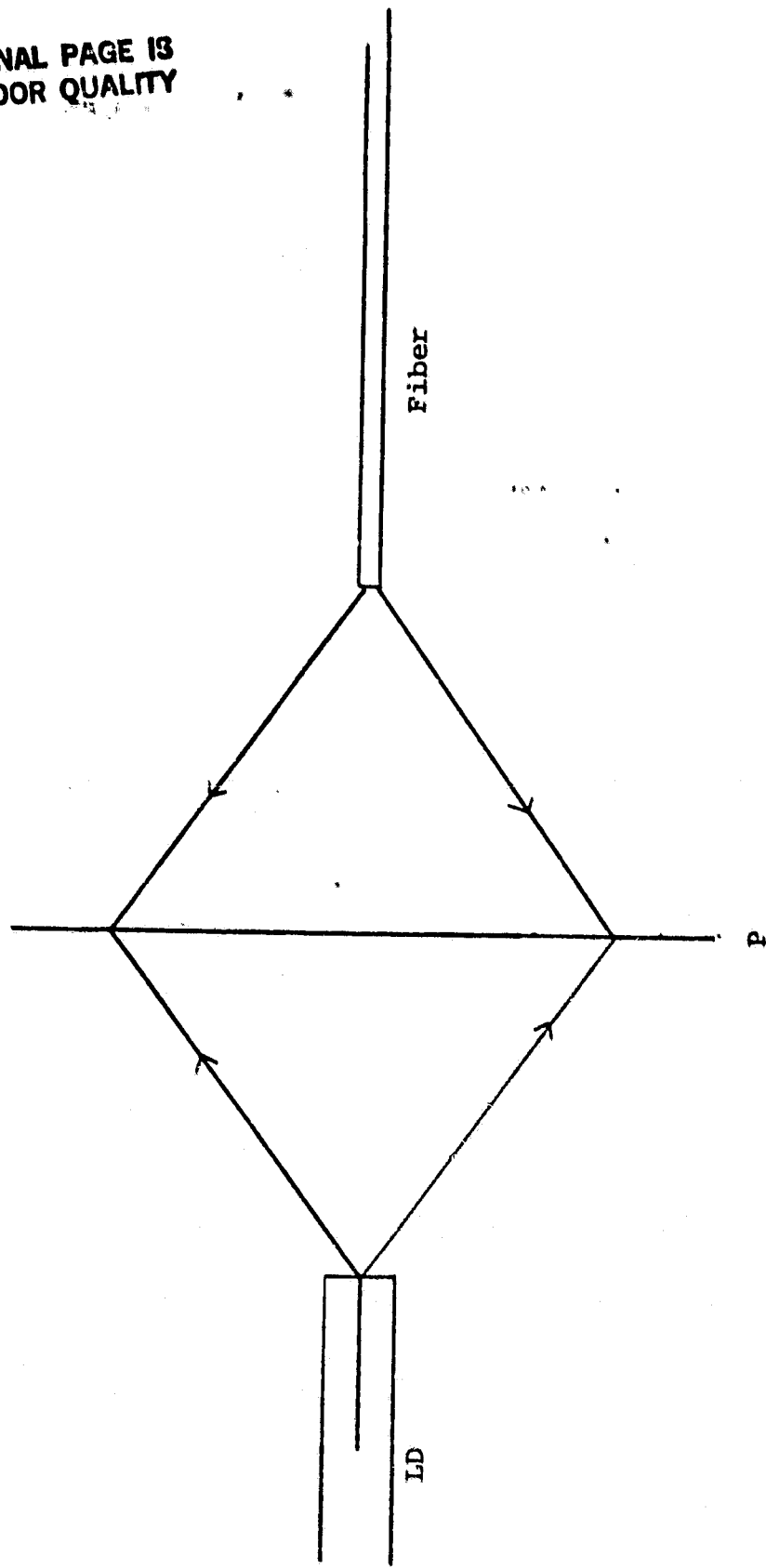


Figure 1. Component positions for superposition of the fields emanating from the LD and the fiber.

ORIGINAL PAGE IS
OF POOR QUALITY

For the case of a monochromatic field:

$$I_p = |U_{LD}(x_0, y_0)|^2 + |U_f(x_0, y_0)|^2 + 2 A(x_0, y_0) a(x_0, y_0) \cos(\Psi(x_0, y_0) - \theta(x_0, y_0))$$

Investigation of the terms yields:

$$|U_{LD}|^2 = \left(\frac{1_x 1_y}{\lambda z} \right)^2 \operatorname{sinc}^2 \left(\frac{1_x y_0}{\lambda z} \right) \operatorname{sinc}^2 \left(\frac{1_y y_0}{\lambda z} \right) \quad (7)$$

$$|U_f|^2 = \left(\frac{K_1}{8z} \right)^2 \left[\frac{2J_1 \left(\frac{K_1 \sqrt{x_0^2 + y_0^2}}{2z} \right)}{\left(\frac{K_1 \sqrt{x_0^2 + y_0^2}}{2z} \right)} \right] \quad (8)$$

$$2A(x_0, y_0) a(x_0, y_0) = 2 \left(\frac{K_1}{8z} \right) \left[\frac{2J_1 \left(\frac{K_1 \sqrt{x_0^2 + y_0^2}}{2z} \right)}{\left(\frac{K_1 \sqrt{x_0^2 + y_0^2}}{2z} \right)} \right]^2 \left(\frac{1_x 1_y}{\lambda z} \right) \operatorname{sinc} \left(\frac{1_y y_0}{\lambda z} \right) \operatorname{sinc} \left(\frac{1_x x_0}{\lambda z} \right) \quad (9)$$

$$\Psi(x_0, y_0) - \theta(x_0, y_0) = K_1 \left(z + \frac{x_0^2 + y_0^2}{2z} \right) - K_2 \left(z + \frac{x_0^2 + y_0^2}{2z} \right)$$

(10)

ORIGINAL PAGE IS
OF POOR QUALITY

so,

$$I_p = \left(\frac{1_x 1_y}{\lambda z} \right)^2 \operatorname{sinc}^2 \left(\frac{1_x x_o}{\lambda z} \right) \operatorname{sinc}^2 \left(\frac{1_y y_o}{\lambda z} \right) + \left(\frac{K_1^2}{8z} \right)^2 \frac{2J_1 \left(\frac{K_1 \sqrt{x_o^2 + y_o^2}}{2z} \right)}{\left(\frac{K_1 \sqrt{x_o^2 + y_o^2}}{2z} \right)} \\ + \frac{K_1^2}{\lambda z} 1_x 1_y \operatorname{sinc} \left(\frac{1_x x_o}{\lambda z} \right) \operatorname{sinc} \left(\frac{1_y y_o}{\lambda z} \right) \frac{2J_1(A)}{A} \quad (11)$$

Figure 2 shows a cross section of I_p ($x_o, y_o = \pi \lambda z / 2ly$) with $\lambda = 830$ nm, $z = 150$ microns, $ly=0.7$ microns, $1x=10$ microns, $1=6$ microns. These plots were generated by the computer program PF.FOR (listed in Figure 13).

III. COUPLING EFFICIENCY

The coupling efficiency, η_c , can be decomposed into two principal terms; the transfer efficiency η_t , and the intrinsic coupling efficiency η_i :

$$\eta_c = \eta_t \eta_i \quad (12)$$

depicted in Figure 3.

The transfer efficiency involves the amount of input radiation absorbed by the hologram and its diffraction efficiency. It has been shown that for thick holograms transfer efficiencies of 85% are quite possible (7). The intrinsic coupling efficiency, η_i , is the ratio of the light power accepted by the fiber to the power incident on the fiber's front facet. Thus η_i

ORIGINAL PAGE IS
OF POOR QUALITY

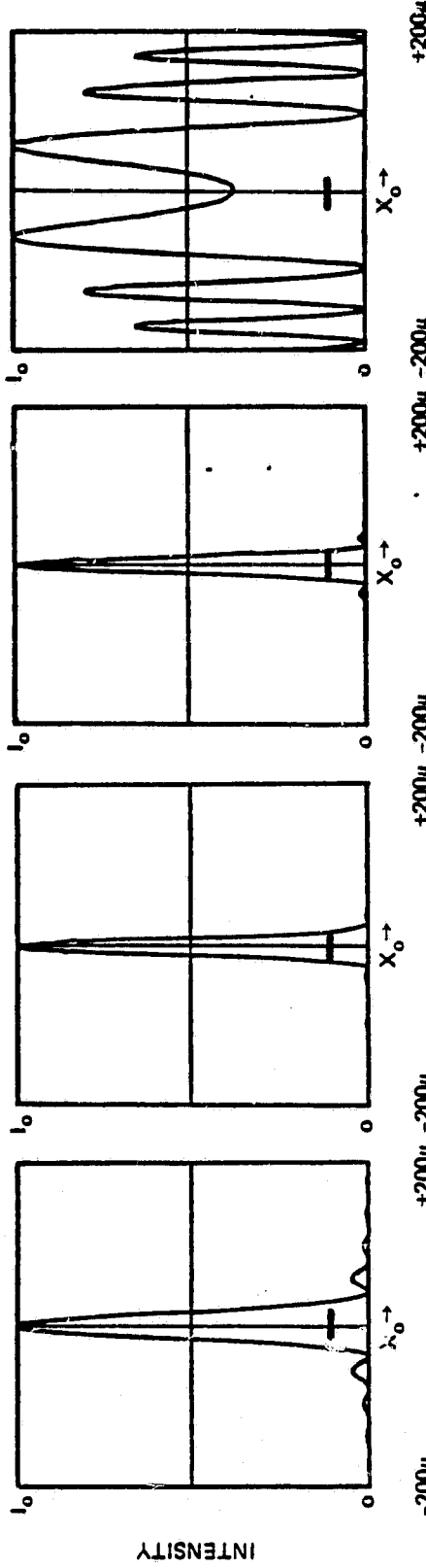


Figure 2. Cross-sectional views of the intensity distribution at the plane P . 2a is the intensity pattern for the rectangular aperture; 2b is for the circular aperture; 2c is the combined intensity pattern on the Y_o axis; 2d is the combined pattern for $Y_o =$.

ORIGINAL PAGE IS
OF POOR QUALITY

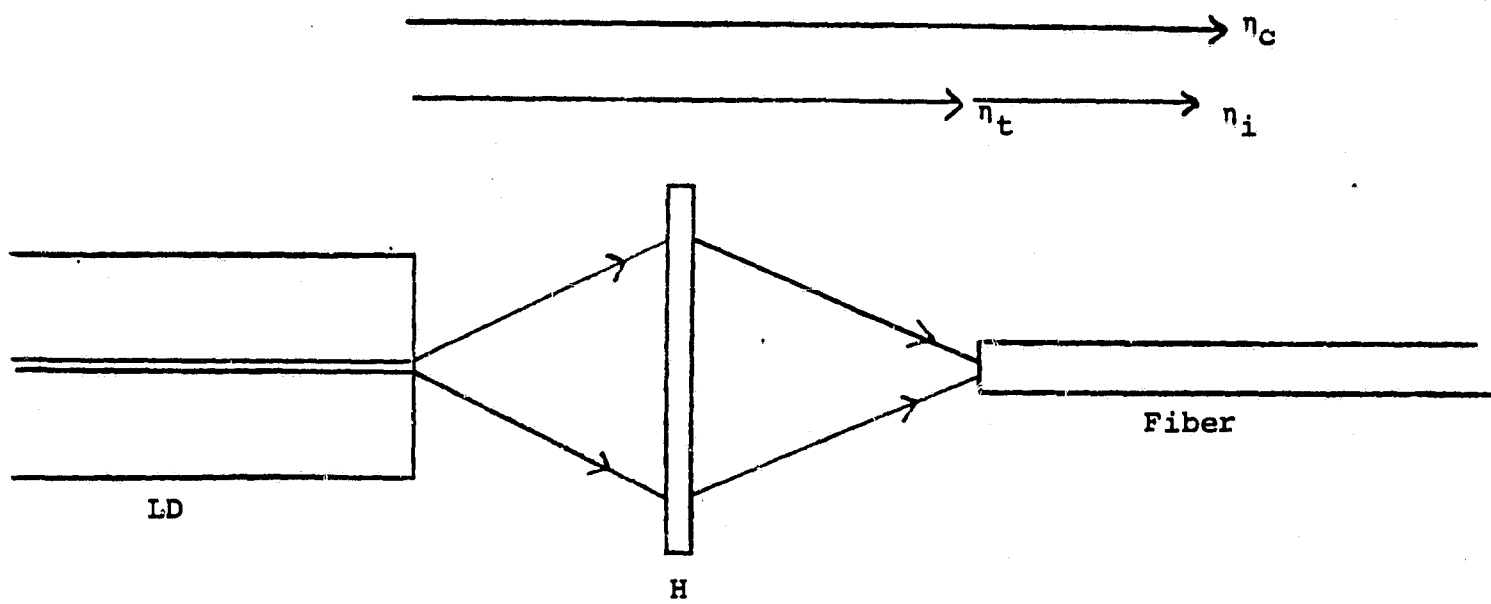


Figure 3. Coupler efficiency defined as the product of the transfer and intrinsic coupling efficiencies.

depends on the accuracy of the hologram's imaging of the fiber's front facet. Leite and Soares (8) have shown that values of n_1 above 85% can be achieved with only moderate difficulty.

Taking these reported values for the respective efficiencies, it should be possible to attain coupling efficiencies, n_c , of approximately 75%.

IV. DOUBLE HOLOGRAM TECHNIQUE

The single element holographic method for coupling, while improving the coupling efficiency, still suffers, like the other coupling schemes, from the severe alignment tolerances. Unlike the other coupling schemes, alignment tolerances can be relaxed by using a slightly revised holographic method.

In this revised holographic method, the single hologram is split into 2 holograms (Figure 4). The first hologram is designed to convert the non-symmetric diverging LD emission into a plane wave. The second hologram is designed to convert an incoming plane wave into the fiber's far-field diffraction pattern (Airy disk). By utilizing the fact that holograms have all of the pattern's information stored in a small area, the alignment sensitivity, with respect to each other, of all four of the components (LD, holograms 1 and 2, and the fiber) is greatly decreased when compared to the sensitivity of the other coupling methods.*

*Lateral displacements between the coupler sections have virtually no consequence. However, tilt and rotation alignment become sensitive ((8) discusses methods for minimizing this sensitivity). Longitudinal displacement between the coupler and the source (LD or fiber) is believed to be no more sensitive than in the traditional techniques (20 microns for 1 dB loss) (4).

ORIGINAL PAGE IS
OF POOR QUALITY

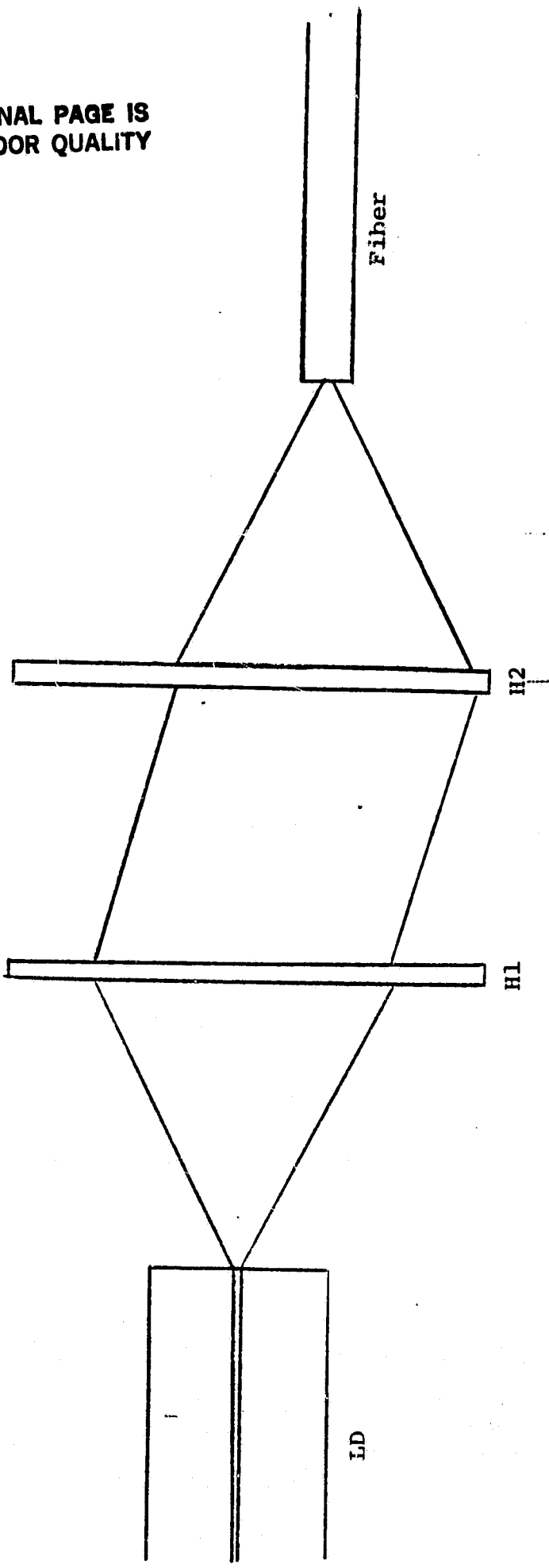


Figure 4. Double Hologram Configuration

V. TWO-BEAM HOLOGRAPHIC FABRICATION

Fabrication of the holographic couplers consists of merely making the hologram(s). For the single element device, the holographic recording scheme employed is depicted in Figure 5a. The reconstruction (coupling) configuration is shown in Figure 5b. In the recording case, light emerges from the LD and interferes on the photographic film/plate P with light from another laser focussed at the spot where the fiber's end facet will be placed.* The plate is then developed and reinserted into the system at plane P. When the hologram is illuminated by the LD radiation, U_{LD} , the fiber's coupling wave, U_f , is generated which propagates into the fiber.

In the case of the double holographic element technique, two holograms are generated. The recording procedure consists of using plane reference waves, U_{r1} and U_{r2} , making complementary angles with the plane of the holograms in conjunction with the LD and fiber emissions (Figure 6). When hologram H1 is illuminated by the radiation from the LD, the plane wave U_{r1} is generated. This wave, in turn, generates the coupling wave U_f^* when it illuminates hologram H2.

VI. COMPUTER GENERATED HOLOGRAMS

A. INTRODUCTION

Another method of fabricating holograms is to use a computer and a plotter. In this method, the two-dimensional intensity distribution resulting

*Notice, in Figure 5A, that the fiber is positioned conjugate to where it will be when LD light is coupled into the fiber (Figure 5b).

ORIGINAL PAGE IS
OF POOR QUALITY

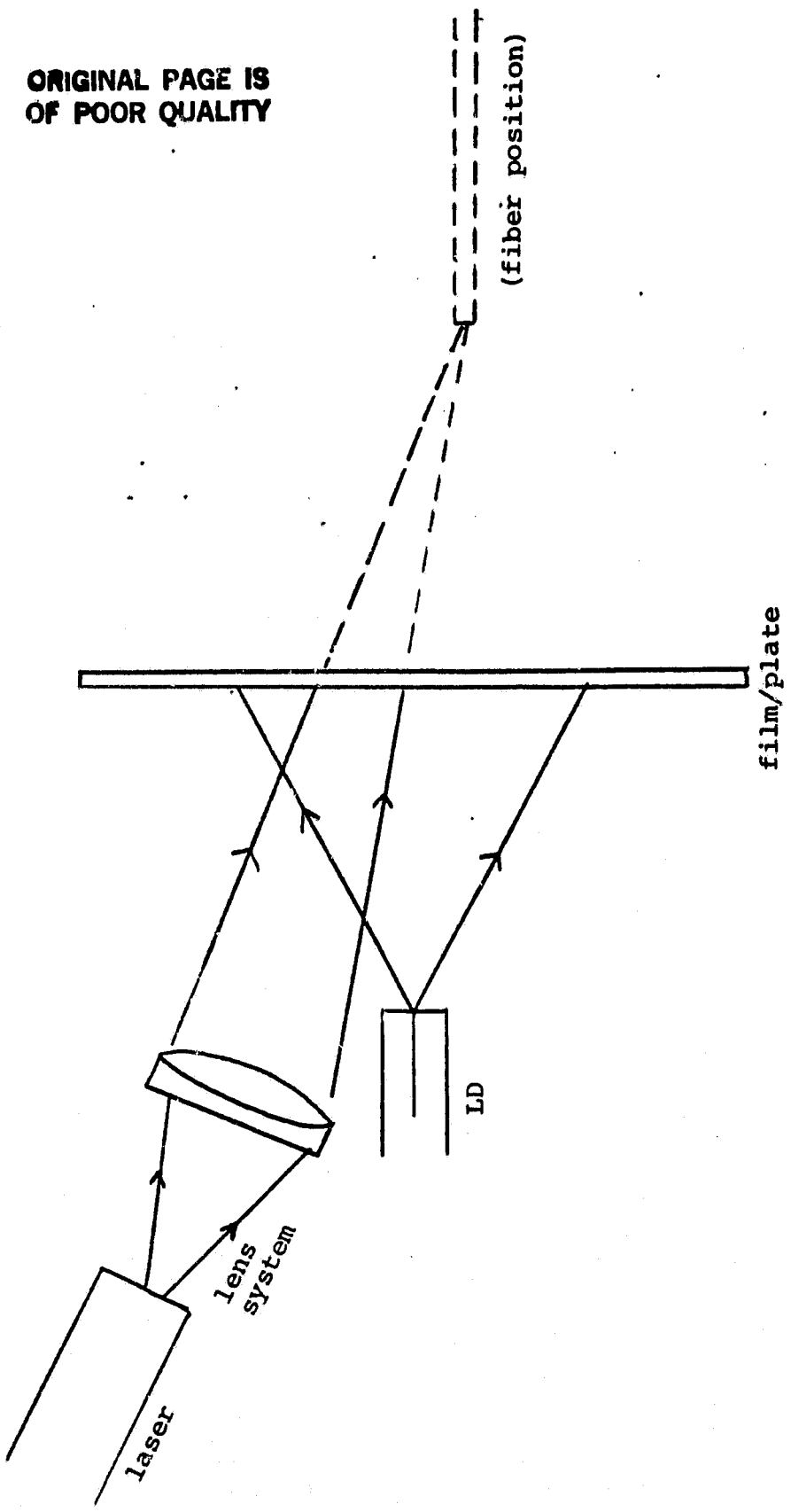


Figure 5a. Recording scheme for the single holographic element coupler.

ORIGINAL PAGE IS
OF POOR QUALITY

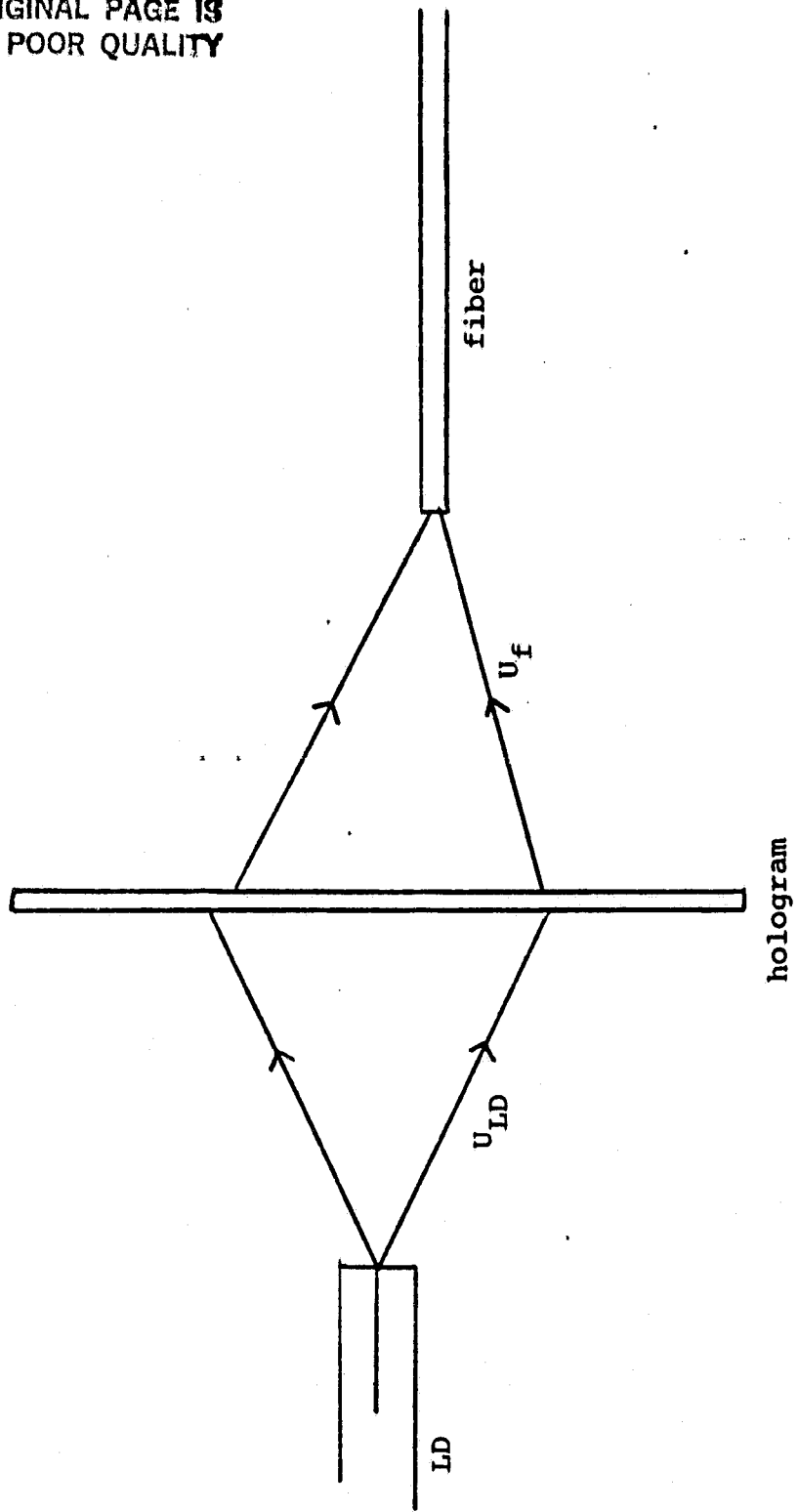


Figure 5b. Reconstruction (coupling) method for the single holographic element coupler.

ORIGINAL PAGE IS
OF POOR QUALITY

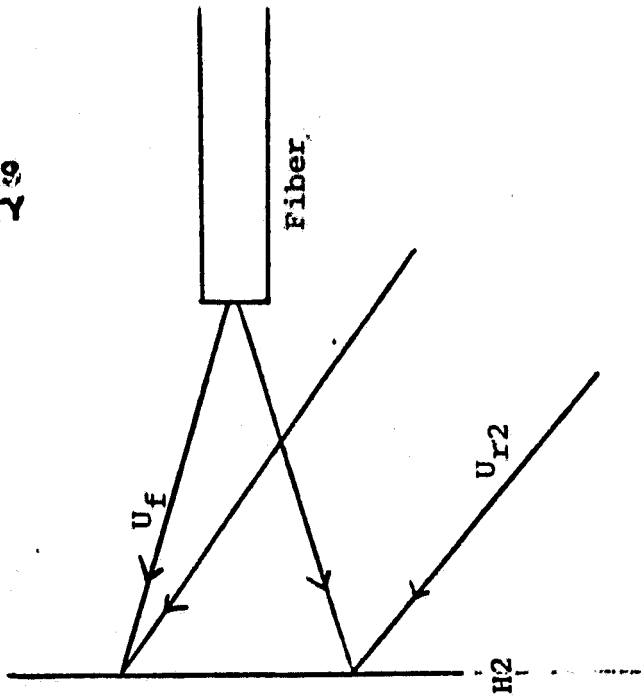


Figure 6. Recording scheme for the double hologram coupler.

from two beams interfering at some plane is calculated. This pattern is then converted into a form suitable for graphical representation by a discrete plotting device. A transparency is formed of the plot photographically or by some other method. The transparency then serves as the hologram.

Calculation of the intensity distribution resulting from the interference of two beams is a straight forward process. The diffraction patterns of the two radiation sources are known, or calculated, for the diffraction region in which they will be used (Fraunhofer or Fresnel). These fields are then propagated to the plane of interference and summed.* The intensity distribution of the interference plane is subsequently calculated.

At this point the hologram's intensity variation is known by the computer. This pattern must then be displayed in a form such that a transparency may be formed. The simplest method of displaying the pattern is to plot it on a hard-copy graphics device. The resulting printout may then be photographed to form the transparency.

The problem becomes one of how to accurately represent the intensity pattern, consisting of phase and amplitude information, by a discrete plotting device.

The most widely used method for displaying phase and amplitude information on a discrete plotting device is Lohmann's technique developed explicitly for computer generated holography (9). A binary (light-dark)

*This plane defines the position between the two devices where the hologram will be placed for reconstruction.

plotting scheme is used since it eliminates the need for generation of gray levels. Another benefit of the binary scheme is that in the photographic reduction step, development procedures are far less critical than for continuous-tone objects.

Lohmann's method utilizes the fact that the phase of the offset reference wave, also used for reconstruction, varies linearly along the x axis.* Consider the system depicted in Figure 7 where a binary mask has been placed in the hologram plane. The mask is primarily opaque with holes centered on a regular grid at the sample points. The linear distance Δx_o is chosen such that the phase of the offset reference wave increases along x by 2π radians through that distance. If two adjacent holes were spaced by Δx_o , then all of the light passed by the two holes will be of the same phase. If, however, one hole is displaced a distance $1.25 \Delta x_o$ from its adjacent one, as with holes C and B in Figure 7, then the light passed by that hole (C) will differ from the adjacent hole (B) by $2\pi + \pi/2 = 5\pi/2 = \pi/2$ radians. Destructive interference will occur between the light from these two holes. This technique of displacing the mask's holes with respect to one another, in accordance with the spacing Δx_o , and thereby encoding the phase of each sample point, is what Lohmann devised. Displacement of the holes is only performed in one direction thereby implying that there be constant phase along the orthogonal axis. The size of the hole corresponds to the amplitude of each sample.

Choosing the linear displacement, Δx_o , which corresponds to a 2π radian phase change of the reference wave establishes the recording, and thus the

*This procedure is applicable for a planes reference wave. This technique would then be suitable for the two-element holographic coupler system, but not for the single element system.

ORIGINAL PAGE IS
OF POOR QUALITY

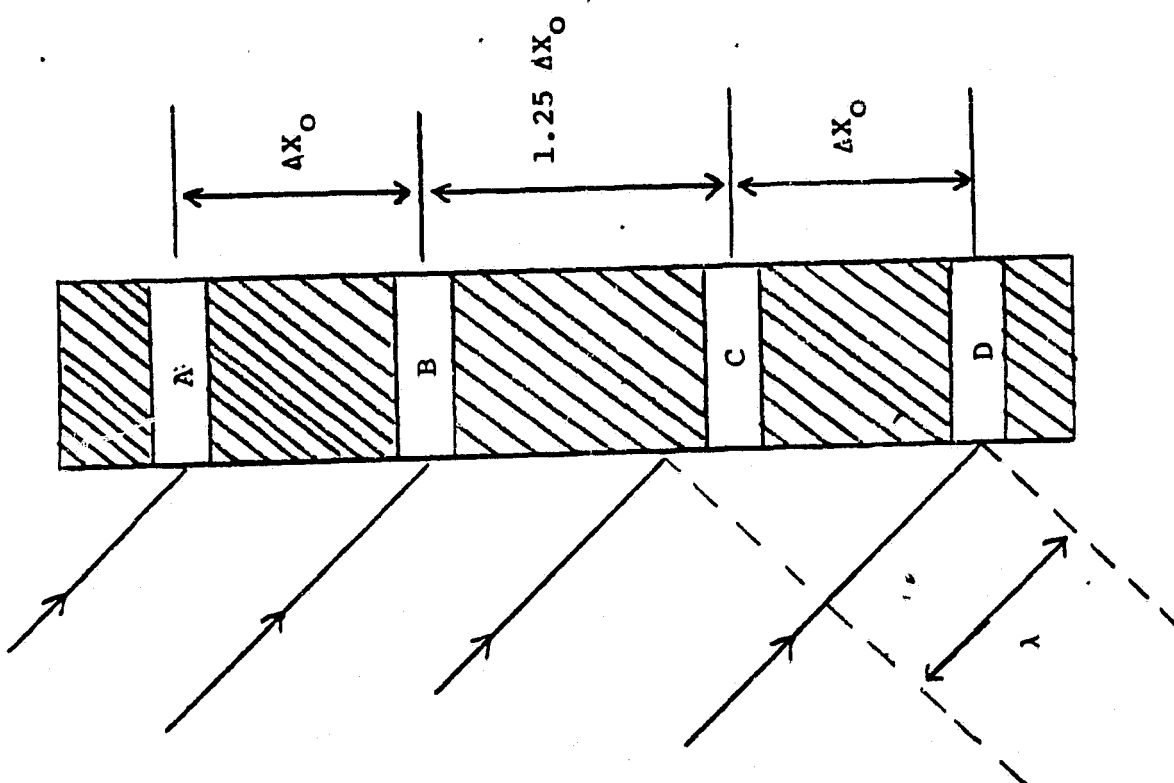


Figure 7. Schematic representation of Lohmann's method.

ORIGINAL PAGE IS
OF POOR QUALITY

reconstruction, angle for the hologram. Figure 8 depicts a plane wave incident on a grid at an angle θ_i . The path difference between the adjacent slits is given by:

$$[\Delta OPL] = d \sin \theta_i \quad (13)$$

The corresponding phase difference is:

$$\delta = \left(\frac{2\pi}{\lambda}\right) d \sin \theta_i \quad (14)$$

We have chosen the linear distance $\Delta z_o = d$ to correspond to a 2π radian phase difference. So:

$$2\pi = \frac{2\pi}{\lambda} \Delta x_o \sin \theta_i \quad (15)$$

The recording and reconstruction angle is then given by:

$$\theta_i = \sin^{-1} \left(\frac{\lambda}{\Delta x_o} \right) \quad (16)$$

The linear displacement distance, Δx_o , is chosen based on, among other things, the resolution of the plotting device, its maximum allowable plotting size, and the number of discrete points in the sample.

B. FOURIER TRANSFORM HOLOGRAMS

Lohmann first examined Fourier transform holograms (i.e. holograms of the Fourier transform of the object rather than of the object itself) (9, 10).

ORIGINAL PAGE IS
OF POOR QUALITY

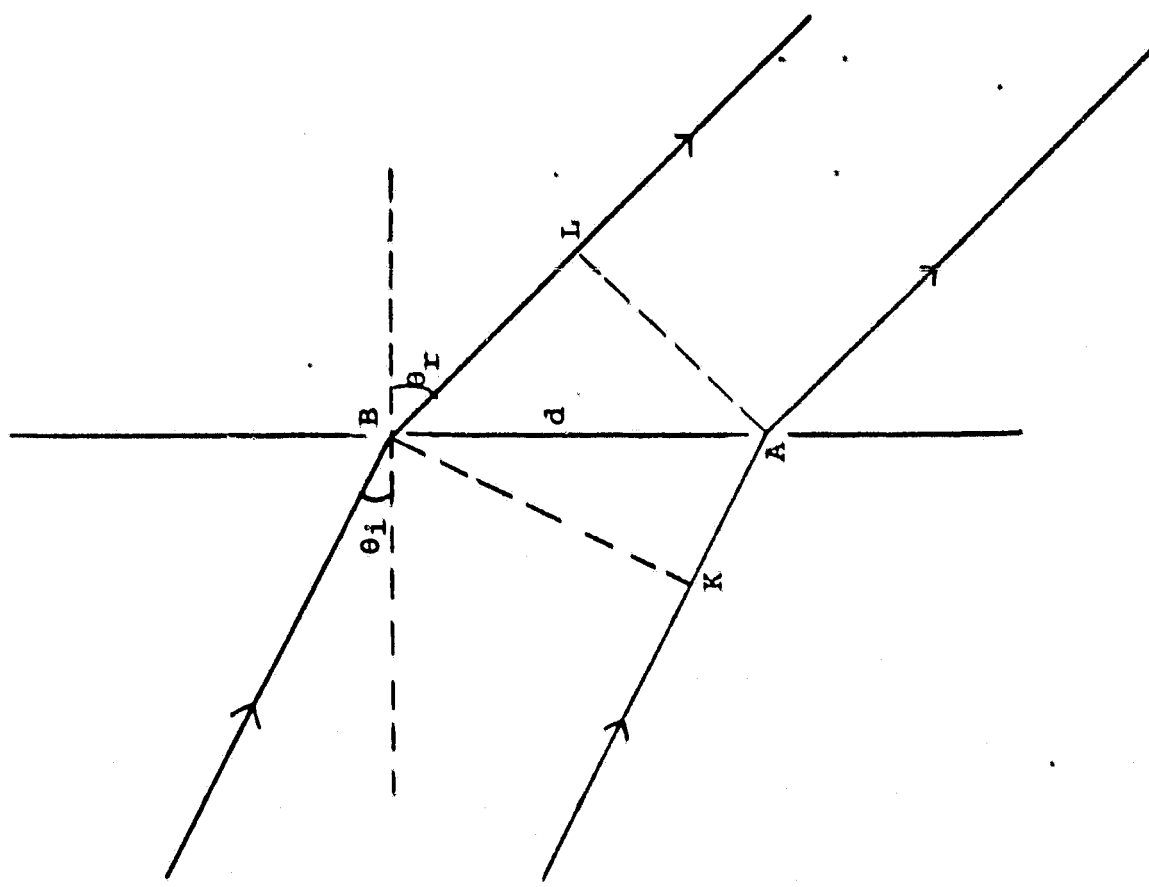


Figure 8. A plane wave incident on a grid.

The method used to generate the hologram relies on the plotting scheme described earlier. The procedure for producing a computer generated Fourier transform hologram is the following. The object, if it is represented by a continuous function, is decomposed into discrete samples so that a FFT may be performed on it numerically. This sampling interval should be chosen in accordance with the Whittaker-Shannon sampling theorem thereby ensuring that the maximum amount of information about the object is retained. The Fourier transform of the object is computed using a discrete FFT routine. Each sample of the Fourier transform of the object is encoded via the Lohmann method. The plot is photographically reduced, negated,* and reconstructed. Reconstruction is accomplished by using a lens to perform an optical Fourier transform of the image formed by the hologram (Figure 9).

C. EXPERIMENT - A COMPUTER GENERATED BINARY FOURIER TRANSFORM HOLOGRAM

A binary computer generated Fourier transform hologram of the two-dimensional character P was produced. A Digital Equipment Corporation VAX-11/780 computer with an associated Trilog printer/plotter was used to perform the computations and plotting. The procedure followed in fabricating the hologram is that outlined earlier. The character was defined in a discrete array of dimensions 64 x 64. By defining the object discretely, the need for accurate sampling of a continuous function was avoided. The Fourier transform of the object was performed by the IBM scientific support FFT subroutine HARM.

*The aperture representing the phase and magnitude of each sample is darkened in. The use of the photographic negative as the hologram reverses the plotted contrast thereby making only the aperture transparent.

ORIGINAL PAGE IS
OF POOR QUALITY

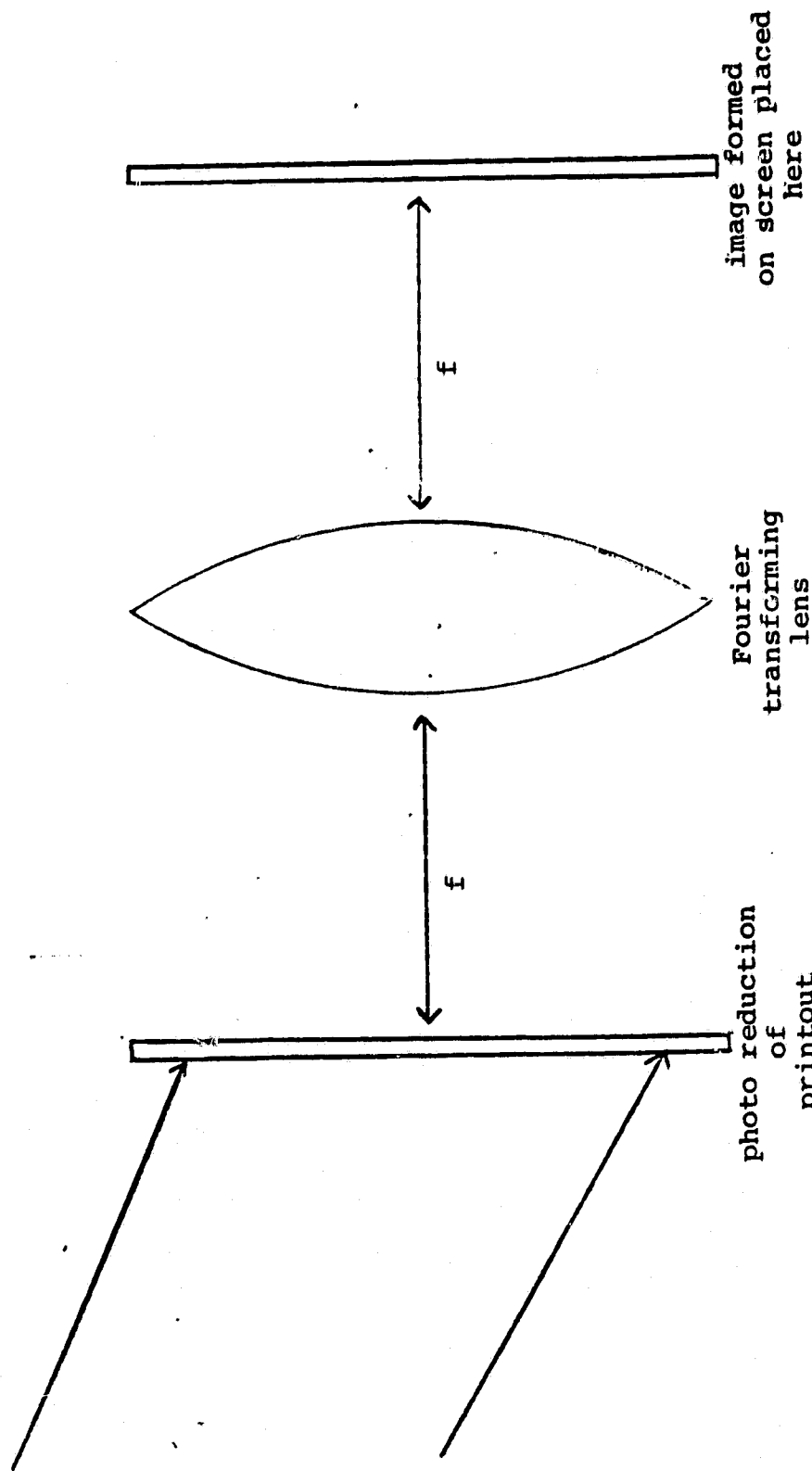
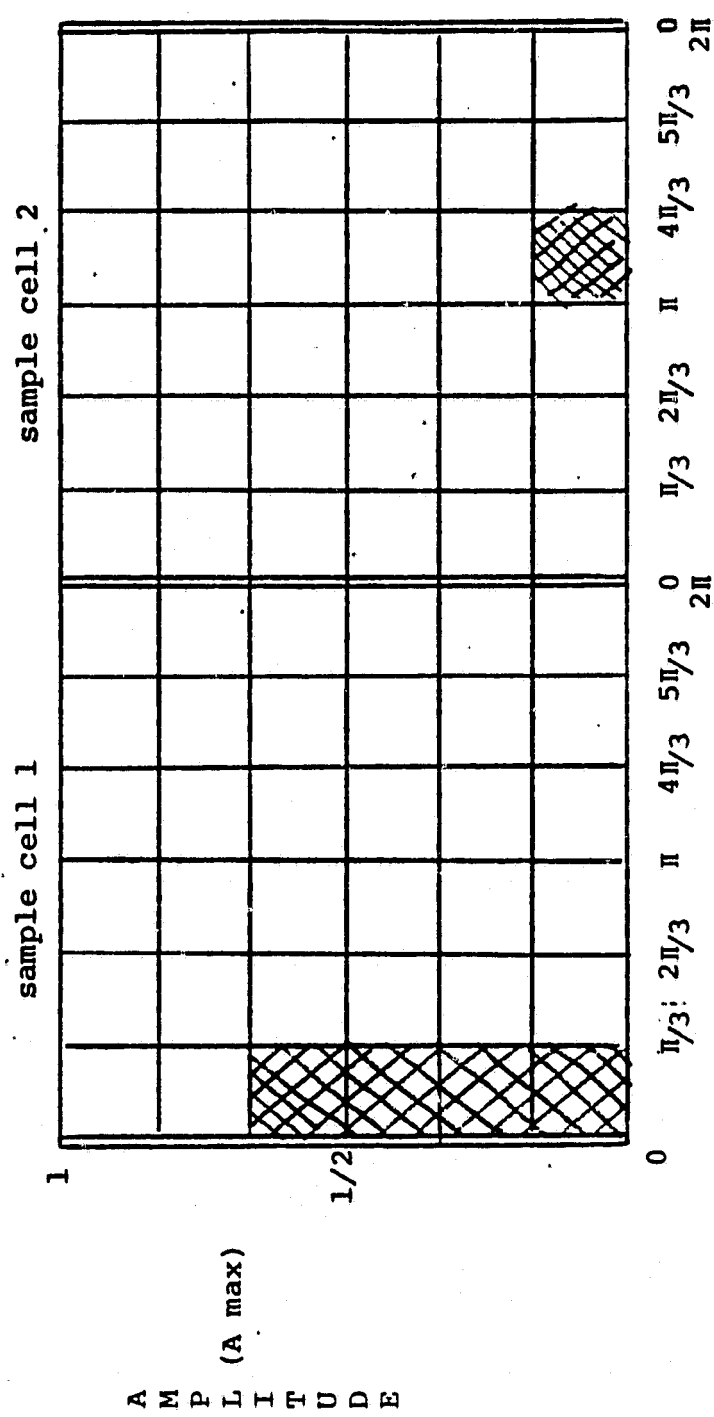


Figure 9. Reconstruction system for a Fourier transform hologram.

Each element in the Fourier transformed object has its phase and magnitude encoded as an aperture within a square cell. The height of the aperture is proportional to the magnitude of the sample, while the position of the aperture within the cell is determined by the sample's phase. The size of the square encoding cell, along with the plotter's resolution, dictate the quantization levels for the phase and magnitude of the sample. Figure 10 depicts two adjacent cells in which the phase and magnitude of two adjacent sample points of Fourier transform of the object will be plotted. The object was represented by a 64×64 element array. The Trilog plotter can plot 1320 points across its 30.48 cm (12 inch) plotting region. The plotter's resolution is therefore 0.0231 cm. At this point, it would be possible to quantize the phase of each element into 20 parts ($1320/64 = 20.62$). While this would allow very good phase representation, the aperture would have a width of 0.0231 cm. This would result in a very dim image because of the narrow aperture. The phase quantization level was chosen as 6 so that each phase region would be represented by 3 pixels.* The aperture width was thus 0.0693 cm. The magnitude quantization level was not limited by the plotter, only by the length of plotting paper available. The magnitude quantization was chosen to be 7. Thus the height of the aperture could range from 0.0 to 0.1386 cm. The linear extent of the square aperture cell (Figure 10) was 0.1386 cm. Since the linear extent of the square cell corresponds to Δx_o , this implies that $\Delta x_o = 0.1386$ cm. Δx_o corresponds to a 2π radian phase change so by equation (16) we see that the recording and reconstruction angle, for He-Ne laser light ($\lambda = 6328$ Å) is 0.0262 degrees.

*While this coarse phase quantization results in some degradation in the reconstructed image, the image brightness was deemed more important at this time.

ORIGINAL PAGE IS
OF POOR QUALITY



$A_1 \leq 2/3 A_{\max}$
 $0 < \phi \leq \pi/3$

$A_2 \leq 1/6 A_{\max}$
 $\pi < \phi \leq 4\pi/3$

Figure 10. Aperture cells for object representation. ΔX_0 corresponds to a 2π radian phase change.

The method for encoding the object's information is to calculate the phase and magnitude of the Fourier transformed object and see what quantization bin each element's values fall into. The phase quantization level of 6 means that the bins span the phases $0-\pi/3$, $\pi/3-2\pi/3$, $2\pi/3-\pi$, $\pi-4\pi/3$, $4\pi/3-5\pi/3$, $5\pi/3-2\pi$. The object element being plotted has its phase scanned and the appropriate phase bin noted. The maximum magnitude in the entire object array is found. This point will have its entire aperture filled in and is therefore scaled to the magnitude quantization level of 7. The magnitude of each object is then scaled to the maximum magnitude value. The magnitude of each element is examined to see how much of the aperture should be filled in. The appropriate magnitude quantization amount is noted. By proceeding through the entire object array, the plot array is determined and plotted.

Figure 11 shows the original object plotted on the phase-magnitude grid. Figure 12 shows the Fourier transform of the object plotted on the phase-magnitude grid. Notice in Figure 12 that the sizes and locations of the apertures differ for different object points.

Initial plotting of the Fourier transformed object showed that the FFT has too large of a dynamic range for quantization into only seven levels. Therefore, the logarithm of the FFTed object was used for magnitude quantization. To avoid arguments of zero, a one was added to each value in the FFT object. The side effect of this operation is to enhance edge detail in the reconstructed image, as low frequencies are suppressed with respect to higher ones (11).

ORIGINAL PAGE IS
OF POOR QUALITY.

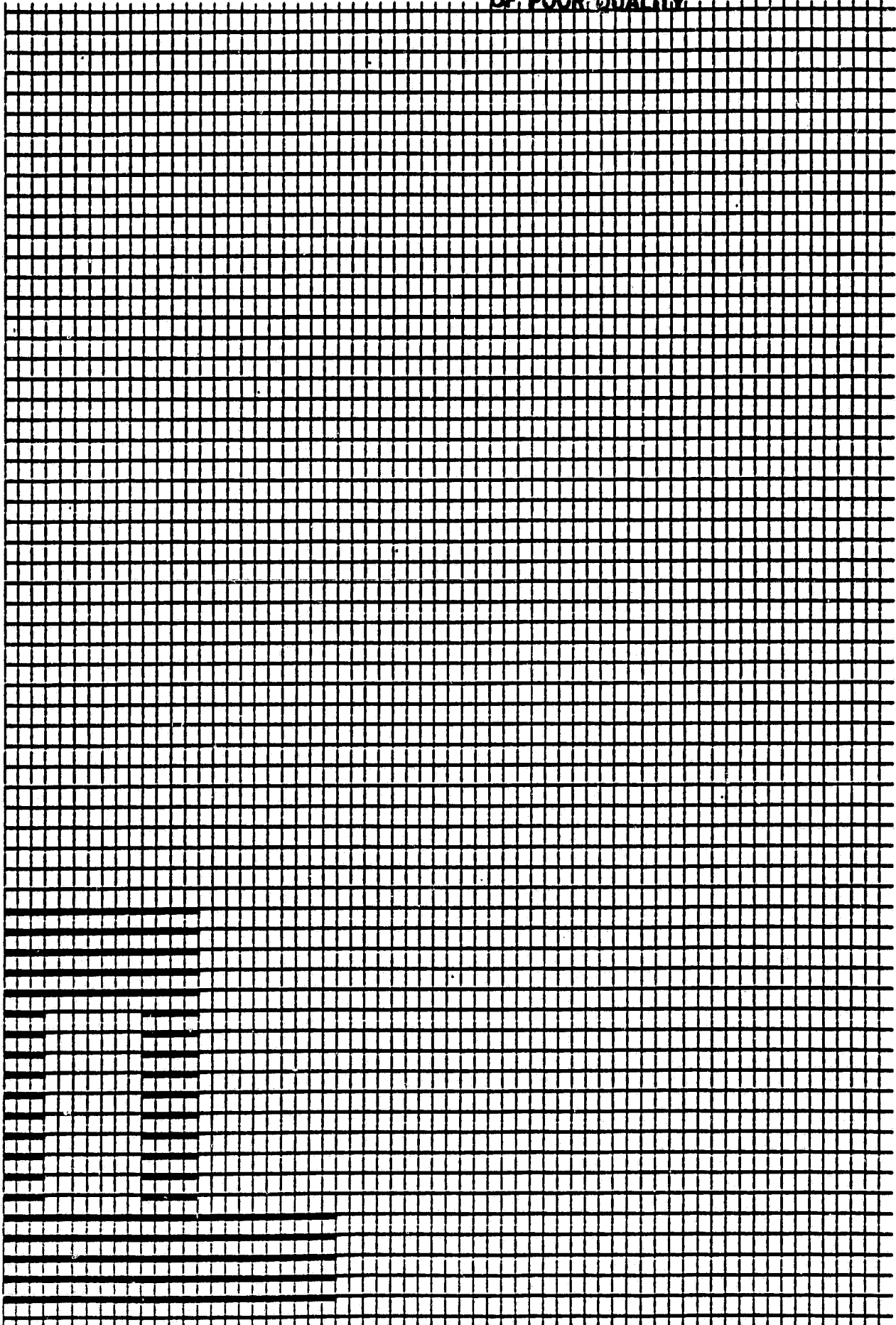


Figure 11. Original object plotted on the phase magnitude grid.

ORIGINAL PAGE IS
OF POOR QUALITY

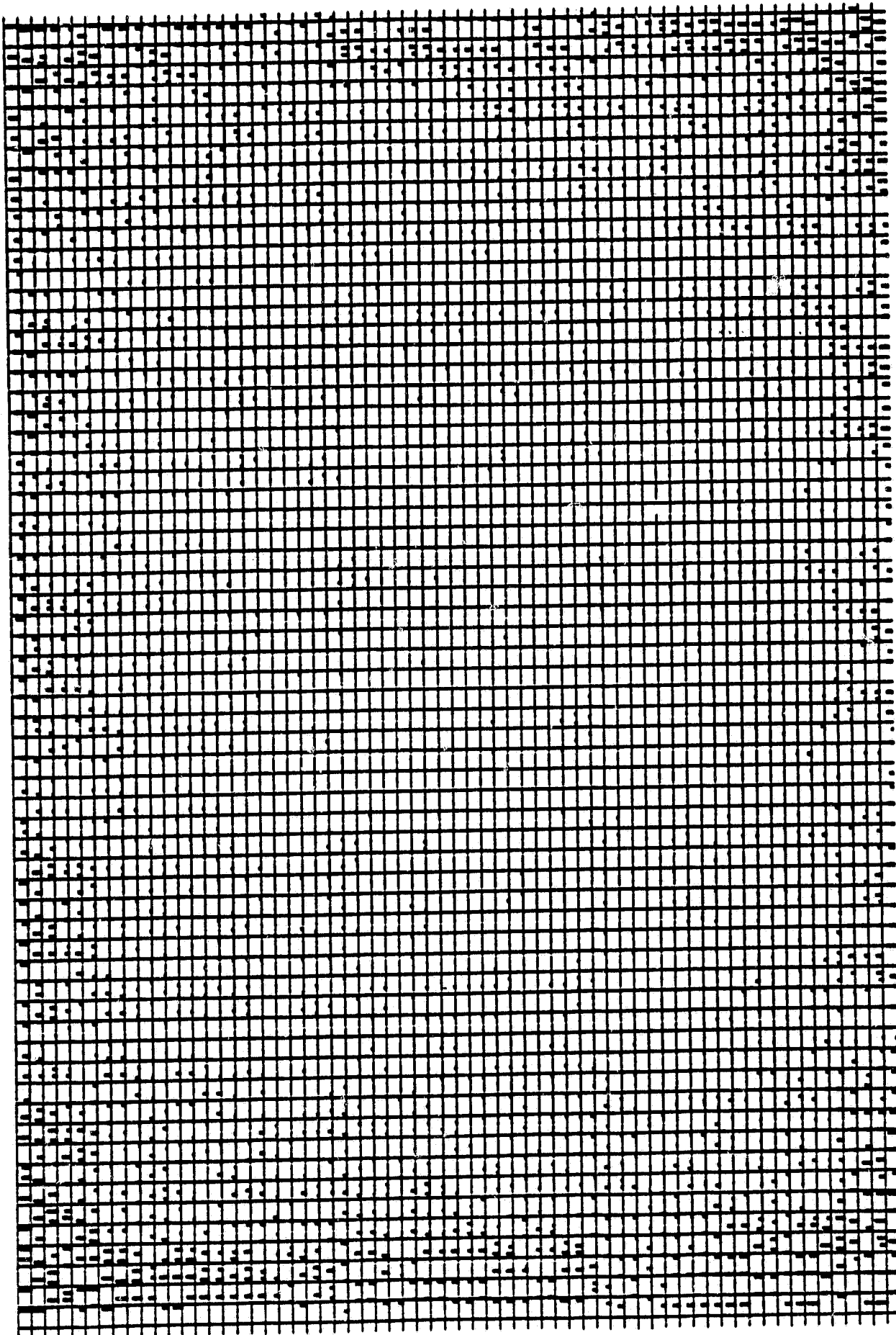


Figure 12. Fourier transform of object plotted on phase-magnitude grid.

A listing of the computer program, CGHBLACKP FOR, used to generate the binary plots is given in Figure 14.

VII. CONCLUSIONS

The use of holographic couplers for LD - fiber systems results in reduced alignment tolerances and higher efficiencies than the traditional techniques used in coupling.

Fabrication of the couplers could be achieved via conventional holographic manufacturing techniques or by the computer generated approach. While both techniques have their advantages, overall the conventionally fabricated hologram is the better of the two when used as coupling devices. The diffraction efficiency from a conventional hologram is higher than from a binary computer generated hologram (12). Considerable higher resolution is obtainable in the conventional fabrication process than in the computer generated process. Holographic films have resolutions of 1250 lines/mm (0.8 microns) (13) while plotting devices resolution is typically 200 microns. While binary computer generated holograms can be fabricated for non-existent devices, a mathematical description of the object is necessary and may be hard to implement on a computer.

Each holographic coupler is fabricated for the particular LD - fiber pair with which it will be used. Spatial variations in the LD output beam change from LD to LD and therefore may not match the recorded LD beam pattern.

There are some limitations in the use of holographic coupling devices. Recording film sensitivity is quite low in the 830 nm wavelength region. This effect requires relatively long exposure times over which the recording system must remain very stable. Fluctuations in the LD output beam due to temperature instability will introduce a mismatching factor into the coupling system. The hologram was developed for one particular LD beam pattern; when the reconstruction beam pattern differs from the recorded beam pattern, LD - fiber matching will degrade.

Overall, the advantages of holographic couplers over the traditional couplers for LD - fiber systems warrant experimentation into the hologram's practical usefulness in coupling.

ORIGINAL PAGE IS
OF POOR QUALITY

C Program: CGHblackP.FOR

C This program generates a Fourier transform plot suitable for
c conversion into a hologram following photographic reduction.
c The Triolog printer/plotter is used for generation of the binary
c plot.

c (CGHblackP plots only black characters. the colored phase-magnitude
c grid is not generated in this program).

c author: P.Fuhr
c date: March - April 1982

```
complex a(64,64,1)          !array containing complex image
complex b(64,64)            !"           " magnitude and phase of
integer iplotm(64),iplotp(64) !this image's FFT
dimension inv(16),s(16)      !phase and magnitude plot arrays
dimension piz(6)             !arrays used by the FFT routine HARM
                                !Pi array ranging from -(2/3)*pi to
                                !pi itself
                                !another array used by HARM
integer m(3)
integer qz
byte plot(222)
common /tridat/plot,mcolor
data m/6,6,0/
data pi/3.1415926/
.
init piz array
pizinc=pi/3.
do 2 j=1,6
  piz(j) = -((65./64.) * pi) + (j*pizinc)
2
cc before anything else, go grab the TRILOG
call tri_init
do 3 j=1,220
  plot(j) = "100
3
  continue
  plot(221)=5
  plot(222)=10
.
do 7 i=1,64
do 7 j=1,64
  a(i,j,1)=cmplx(0.0,0.0)
  b(i,j)=cmplx(0.0,0.0)
7
  continue
.
f the character 'P'
c define the character in the array 'a'
.
do 20 i=1,3
do 10 j=1,20
  a(i,j,1)=cmplx(1.0,0.0)
20
10
```

ORIGINAL PAGE IS
OF POOR QUALITY

```

10      continue
20      continue

do 40 i=4,10
do 25 j=1,5
a(i,j,1)=cmplx(1.0,0.0)
25      continue

do 30 j=16,20
a(i,j,1)=cmplx(1.0,0.0)
30      continue
40      continue

do 60 i=11,14
do 45 j=1,20
a(i,j,1)=cmplx(1.0,0.0)
45      continue
60      continue

do 80 i=15,24
do 65 j=1,5
a(i,j,1)=cmplx(1.0,0.0)
65      continue
c      !the character P have been defined in 'a'
80      continue

c      CGHBLACK produces output in black only
c      mcolor=1      !yellow ribbon
c      call tri_color      !change ribbon
c
c      no need for the grid
c
c      do 77 k=1,64
c      do 71 i=1,195
c71      plot(i)="177"      !every bit on
c
c      call tri_dump      !plot this line
c
c      do 73 i=1,220
c73      plot(i)="100"      !every bit off
c
c      do 74 i=2,195,3
c74      plot(i)="120"      !every 6th horizontal space is a vertical line
c      !!(i.e. every 3rd byte ="120)
c
c      do 75 i=1,11
c75      call tri_dump      !11 times
c
c      continue      !every array row
c
c      mcolor=3      !blue ribbon
c      call tri_color      !change ribbon color
c
c      call tri_top

type *,* enter o to plot original, f for FFT, i for Finv(F)
88      accept 88,qz
      format(1a1)

ierr=0      !init HARM error flag

```

ORIGINAL PAGE IS
OF POOR QUALITY

```

c      ifset=1      !have HARM generate its own internal sine
c      !and cosine tables for the FFT
c
c      if(qz.eq.'o')goto 85      !if requested, don't do the FFT
c
c      call HARM(a,m,inv,s,ifset,ierr) !SSP FFT routine
c
c      if(ierr.eq.0)goto 83
c      type *, ' FFT error code *',ierr
c
83      if(qz.ne.'l')goto 85      !don't perform Finv unless requested
c      ifset=-1      !have HARM generate its own internal sine
c      !and cosine tables for F inverse
c
c      call HARM(a,m,inv,s,ifset,ierr) !SSP FFT routine
c      if(ierr.eq.0)goto 85
c      type *, ' inverse FFT error code *',ierr
c
c      determine the magnitude and phase of each object element
c
85      do 100 i=1,64
c      do 100 j=1,64
c      amag=cabs(a(i,j,1))      !find the element's magnitude
c      if(real(a(i,j,1)).ne.0.0)goto 90      !does the real part equal 0?
c      x*pi/2.
c      y*aimag(a(i,j,1))      !get the imaginary component
c      alpha=sign(x,y)      !the phase = pi/2 times the sign (+ or -) of
c      !the imaginary part. (If the real component of
c      !this number =0, then the phase angle is + or
c      !- pi/2. if the imaginary part is negative
c      !then the phase angle is negative.
c
c      goto 95
c
90      alpha=atan2(aimag(a(i,j,1)),real(a(i,j,1)))      !determine the phase angle
c
95      b(i,j)=cmplx(amag,alpha) !put the magnitude and phase into the real
c      !and imaginary parts of b
c
100      continue
c
c      type *, ' do you want to store the mag-phase data (y or n)?'
c      accept 88,qz
c      if(qz.ne.'y')goto 104
c      do 110 i=1,64
c      do 107 j=1,64
c      zmag=real(b(i,j))      !real part (magnitude)
c      zpha=aimag(b(i,j))      !complex part (phase)
c      write(9,1005)i,j,zmag,zpha
c      format(' b(',i2,',',i2,')= ',e15.8,3x,e15.8)
c
1005    107      continue
c
110      continue
c
c      find the maximum magnitude value in the b array
104      zmax=log(real(b(1,1))+1.0)      !make the 1st element the largest (start)
c      !take logarithm because FFT has too large of a dynamic range
c      do 120 i=1,64
c      do 120 j=1,64      !check every element
c      z=log(real(b(i,j))+1.0)
c      zmax=max1(z,zmax)      !use the maximum value function for the
c      !comparison
c
120      continue

```

ORIGINAL PAGE IS
OF POOR QUALITY

```
c      there are 7 levels of magnitude quantization
zmlevel=zmax/7.0

c      there are 6 levels of quantization for the phase
zlevel=6

c      determine the phase quantization of each element
144  do 500 j=1,64

      do 200 j=1,64
      p=imag(b(j,j))      !get the phase
      if(p.lt.piz(1)) iplotp(j)=1
      if(p.ge.piz(1).and.p.lt.piz(2)) iplotp(j)=2      !determine
      if(p.ge.piz(2).and.p.lt.piz(3)) iplotp(j)=3      !which
      if(p.ge.piz(3).and.p.lt.piz(4)) iplotp(j)=4      !segment the phase
      if(p.ge.piz(4).and.p.lt.piz(5)) iplotp(j)=5      !should be encoded in.
      if(p.ge.piz(5)) iplotp(j)=6

c      determine the proper amplitude quantization level for each element
      amag=log(real(b(1,j))+1.0)      !get the magnitude
      zlevel=amag/zmlevel      !scale the data
      if(zlevel.lt.1.0) iplotm(j)=0
      if(zlevel.ge.1.0.and.zlevel.lt.2.0) iplotm(j)=1
      if(zlevel.ge.2.0.and.zlevel.lt.3.0) iplotm(j)=2
      if(zlevel.ge.3.0.and.zlevel.lt.4.0) iplotm(j)=3
      if(zlevel.ge.4.0.and.zlevel.lt.5.0) iplotm(j)=4
      if(zlevel.ge.5.0.and.zlevel.lt.6.0) iplotm(j)=5
      if(zlevel.ge.6.0) iplotm(j)=6      !the largest magnitude

200  continue

cc  next, map this plotting data into the output plot lines (6 plot
cc  lines per 1 array line).
c
c      do 410 k=1,6
      llevel=7-k
      do 400 j=1,64

      scan a plot line
      if(iplotm(j).lt.llevel) goto 400 !go on to next array element

c      there is something to be plotted on this line, find the phase position
      l=3*j
      if(iplotp(j).eq.1) plot(l+1)="170
      if(iplotp(j).eq.2) plot(l+1)="107
      if(iplotp(j).eq.3) plot(l+2)="170
      if(iplotp(j).eq.4) plot(l+2)="107
      if(iplotp(j).eq.5) plot(l+3)="170
      if(iplotp(j).eq.6) plot(l+3)="107

400  continue

c      plot out this line
      call tri_dump      !2 vertical lines per amplitude quantization
      call tri_dump      !level. (12 lines per array row).

      do 405 k1=1,220
      plot(k1)="100      !reset the plot array
405  continue
```

**ORIGINAL PAGE IS
OF POOR QUALITY**

410 continue

500 continue

stop
end

ORIGINAL PAGE IS
OF POOR QUALITY

PROGRAM NAME: PF.FOR

This program calculates the intensity for two electric fields interfering at a plane z distance z between them. Fields are calculated for a rectangular aperture and a circular aperture. These fields are then combined at the holographic (interference) plane. The resulting intensity pattern is subsequently scanned for its maximum value. The output data is scaled such that the maximum value will just saturate the output plot. Plotting is performed on a DEC VT-11 display and a Versatec printer/plotter.

author: P. Fuhr
date: April 1982

```
REAL*4 AVAL(1024),outx(1024),outy(1024)
DIMENSION IBUF(6000)
LOGICAL*1 STRNG(21),aa
real*4 lx,ly,l,lambda,z,pi,kz

CALL INIT(IBUF,6000)           !init graphics display

c acquire user input
type *, ' enter xzero endpoint (in microns)'
accept *,xoend
type *, ' a symmetric graph will be generated'
xosrt = 1.e-6                 !start near zero

c we will generate 512 points the other 512 points come from the
c symmetry of the system
xoinc = (xoend - xosrt)/512.

type *, ' enter constants (all lengths are in microns)'
type *, ' enter x dimension of rectangular aperture'
accept *,lx
type *, ' enter y dimension of rectangular aperture'
accept *,ly
type *, ' enter diameter of fiber core'
accept *,l
type *, ' enter wavelength of light'
accept *,lambda
type *, ' enter distance between apertures and interference plane'
accept *,z

c all lengths are in MICRONS
pi=3.14158

Kz=(2.*pi)/lambda           !propagation constant
zzero = (pi * lambda * z) / (2. * ly)
xzero=xosrt
noff=512                     !internal array offset
```

ORIGINAL PAGE IS
OF POOR QUALITY

```
TYPE *,' input Yzero value (y or n)'  
accept 987,aa  
if(aa.ne.'y'.and.aa.ne.'Y')goto 87  
type *,' enter Yzero'  
accept *,yzero  
  
87  do 600 i=1,512      !calculate the intensity at each point  
type *,i      !let the operator know what point you're on.  
call rect(answer,z,ix,ly,lambda,xzero,yzero)  !rect aperture  
call circ(answr2,z,l,Kz,xzero,yzero)      !circular aperture  
  
first = answer * answer      !square the field  
second = answr2 * answr2    !square the field  
third = 2. * answer * answr2  !cross term  
aval(itwoff) = first + second + third  !sum all components  
xzero = xzero + xoinc      !increment output field position  
600  continue  
  
C      now fill the beginning of the array  
nn=1024  
do 605 i=1..512  
sval(i)=aval(nn-i)  
605  continue.  
  
N3=0  
  
C      FIND MAX. VALUES IN ARRAYS  
AMAX=0.  
amin = 1.e10  
DO 1 K=1,1024  
IF (ABS(AVAL(K)).GT.AMAX) AMAX=ABS(AVAL(K))  
if(aval(k).lt.amin) amin = aval(k)  
1  CONTINUE  
  
type *,' print data (y or n)?'  
accept 987,aa  
987  format(1a1)  
if(aa.ne.'y'.and.aa.ne.'Y')goto 16  
do 73 i=1,1024  
print 933,i,aval(i)  
73  format(2x,i4,2x,e16.8)  
continue  
print 934,amax,amin  
934  format(' AMAX= ',e16.8,' AMIN= ',e16.8)  
  
C      SIZE THE SCREEN, DRAW BORDER  
16  CALL SIZE(7.5,7.5)  
CALL SCAL(0.,0.,72.,72.)  
CALL AXES(0.,0.,72.,72.)  
CALL PLOT1  
if(amax.ne.0.)goto 17  
amax=1.
```

ORIGINAL PAGE IS
OF POOR QUALITY

```
c      vscale=0.  
17      soto 18  
18  
c      scale the data to AMAX and AMIN  
17      vscale = 70./amax  
18      xscale=60./1024.  
do 23 i=1,1024  
outy(i)=avol(i)*yscale      !can't forget the y axis offset  
outx(i)=float(i)*xscale +10.  !or the x axis offset  
23      continue  
  
c      plot out the data  
DO 30 i=1,1024  
x=outx(i)  
y=outy(i)  
call splot(x,y,0,8)  
30      CONTINUE  
  
C      LABEL GRAPH  
TYPE 3  
3      FORMAT(' X-AXIS LABEL?')  
CALL GETSTR(5,STRNG,20,ERR)  
m=0          !horizontal label  
X=40.  
Y=7.  
CALL PLOT2(STRNG,X,Y,m)  
TYPE 4.  
4      FORMAT(' Y-AXIS LABEL?')  
CALL GETSTR(5,STRNG,20,ERR)  
X=10.  
m=1          !vertical label  
Y=50.  
CALL PLOT2(STRNG,X,Y,m)  
  
TYPE 6  
5      FORMAT(X,'COPY:  0=NO,1=YES?')  
ACCEPT *, N1  
IF(N1)15,15,11  
11      CALL PLOT  
      CALL DONE  
  
15      STOP  
      END  
  
C      SUBROUTINE TO DRAW BOARDER  
C  
SUBROUTINE PLOT1  
call splot(10.,0.,0.,-8) !lower left  
call vect(0.,70.)      !left vertical  
call splot(70.,0.,0.,-8) !lower right  
call vect(0.,70.)      !right vertical
```

```

call apnt(10.,0.,0,-8) !lower left
call vect(60.,0.) !bottom
call apnt(10.,70.,0,-8) !upper left
call vect(60.,0.) !top
call apnt(10.,35.,0,-8) !middle left
call vect(60.,0.) !horizontal axis
call apnt(40.,0.,0,-8) !middle bottom
call vect(0.,70.) !vertical axis
return
END

```

ORIGINAL PAGE IS
OF POOR QUALITY

```

C   SUBROUTINE TO DRAW TEXT
C
C   SUBROUTINE PLOT2(STRNG,X,Y,M)
LOGICAL*1 STRNG(21)
L=LEN(STRNG)
IF(M.EQ.1) GO TO 22
C   HORIZ. TEXT
C=X-L/2.
CALL HTXT(C,Y,L,STRNG)
GO TO 24
C   VERT. TEXT
22  C=Y-L/2
CALL APNT(X,C,0,-8)
CALL VTXT(X,C,L,STRNG)
23  CONTINUE
24  RETURN
END

```

```

subroutine rect(answer,z,lx,ly,lambda,xzero,yzero)
implicit real*4 (a-l,o-z)
c   compute the far-field due to a rectangular aperture
c   calculate the amplitude constants
if(lx.ne.0.0.and.ly.ne.0.0)goto 5
answer=0.0
return
5   a = (lx * ly) / (lambda * z)
if(yzero.eq.0.0)yzero=1.e-5
sincy = sin(yzero) / yzero
x0arg = (lx * xzero) / (lambda * z)
if(x0arg.eq.0.0)x0arg=1.e-5
sincx = sin(x0arg) / x0arg
answer = a * sincx * sincy
return
end

subroutine circ(answr2,z,l,kz,xzero,yzero)
compute the far-field out of a circular aperture
implicit real*4 (a-z)
if(l.ne.0.0.and.kz.ne.0.0)goto 5

```

ORIGINAL PAGE IS
OF POOR QUALITY

```

5      answer2=0.0
      return
      b = (Kz * 1 * 1) / (8. * z)
      K12z = (Kz * 1) / (2. * z)
      besars = (xzero * xzero) + (yzero * yzero)
      besars = K12z * sqrt(besars)
      answer2 = (2. * b / besars) * bessel(besars)
      return
      end

c      function bessel(x)
c      compute the Bessel function of the first kind - first order
c      by using the scientific subroutine Packaged program BESJ.FOR
c      z=x           !argument of the Bessel function
c      n=1           !1st order Bessel function
c      d=.01         !accuracy desired
c      call besj(z,n,xj,d,ier)
c      if(ier.eq.0)goto 10           !check for errors
c      bessel = 0.
c      goto(1,2,3,4)ier           !type the corresponding error message
1      type *, ' order of Bessel function less than zero'
c      return
2      type *, ' Bessel argument negative or zero'
c      return
3      type *, ' required accuracy of 0.007 not obtained'
c      return
4      type *, ' range of Bessel order not correct (see SSP doc F.3-35)'
c      return
10     bessel = xj           !return with the answer
c      return
c      end

c      .....
c
c      SUBROUTINE BESJ
c
c      PURPOSE
c          COMPUTE THE J BESSSEL FUNCTION FOR A GIVEN ARGUMENT AND ORDER
c
c      USAGE
c          CALL BESJ(X,N,BJ,D,IER)
c
c      DESCRIPTION OF PARAMETERS
c          X -THE ARGUMENT OF THE J BESSSEL FUNCTION DESIRED
c          N -THE ORDER OF THE J BESSSEL FUNCTION DESIRED
c          BJ -THE RESULTANT J BESSSEL FUNCTION
c          D -REQUIRED ACCURACY
c          IER-RESULTANT ERROR CODE WHERE
c              IER=0 NO ERROR
c              IER=1 N IS NEGATIVE

```

ORIGINAL PAGE IS
OF POOR QUALITY

C IER=2 X IS NEGATIVE OR ZERO
C IER=3 REQUIRED ACCURACY NOT OBTAINED
C IER=4 RANGE OF N COMPARED TO X NOT CORRECT (SEE REMARKS)

C REMARKS

C N MUST BE GREATER THAN OR EQUAL TO ZERO, BUT IT MUST BE
C LESS THAN
C $20+10*X-XXX$ 2/3 FOR X LESS THAN OR EQUAL TO 15
C $90+X/2$ FOR X GREATER THAN 15

C SUBROUTINES AND FUNCTION SUBPROGRAMS REQUIRED

C NONE

C METHOD

C RECURRENCE RELATION TECHNIQUE DESCRIBED BY H. GOLDSTEIN AND
C R.M. THALER, 'RECURRENCE TECHNIQUES FOR THE CALCULATION OF
C BESSSEL FUNCTIONS', M.T.A.C., V.13, PP.102-108 AND I.A. STEGUN
C AND M. ABRAMOWITZ, 'GENERATION OF BESSSEL FUNCTIONS ON HIGH
C SPEED COMPUTERS', M.T.A.C., V.11, 1957, PP.255-257

C
C SUBROUTINE BESJ(X,N,BJ,D,IER)

BJ=.0
IF(N)10,20,20
10 IER=1
RETURN
20 IF(X)30,30,31
30 IER=2
RETURN
31 IF(X-15.)32,32,34
32 NTEST=20.+10.*X-X** 2/3
GO TO 36
34 NTEST=90.+X/2.
36 IF(N-NTEST)40,38,38
38 IER=4
RETURN
40 IER=0
N1=N+1
BPREV=.0

C COMPUTE STARTING VALUE OF M

IF(X-5.)50,60,60
50 MA=X+6.
GO TO 70
60 MA=1.4*X+60./X
70 MB=N+IFIX(X)/4+2
MZERO=MAX0(MA,MB)

C SET UPPER LIMIT OF M

```

      MMAX=NTEST
100 DO 190 M=hZERO,MMAX,3
C
C      SET F(M),F(M-1)
C
      FM1=1.0E-28
      FM=.0
      ALPHA=.0
      IF(M-(M/2)*2)120,110,120
110 JT=-1
      GO TO 130
120 JT=1
130 M2=M-2
      DO 160 N=1,M2
      MK=M-N
      BMK=2.*FLOAT(MK)*FM1/X-FM
      FM=FM1
      FM1=BMK
      IF(MK-N-1)150,140,150
140 BJ=BMK
150 JT=-JT
      S=1+JT
160 ALPHA=ALPHA+BMK*S
      BMK=2.*FM1/X-FM
      IF(N)180,170,180
170 BJ=BMK
180 ALPHA=ALPHA+BMK
      BJ=BJ/ALPHA
      IF(ABS(BJ-BPREV)-ABS(D*BJ))200,200,190
190 BPREV=BJ
      IER=3
200 RETURN
      END

```

ORIGINAL PAGE IS
OF POOR QUALITY

References

ORIGINAL PAGE IS
OF POOR QUALITY

1. C.C. Timmerman, *Appl. Opt.*, 15, 2432(1976).
2. M. Saruwatari and K. NawataK, *Appl. Opt.*, 18, 1847(1979).
3. L.G. Cohen and M.V. Schneider, *Appl. Opt.*, 13, 1021(1974).
4. M. Saruwatary and T. Susie, *IEEE JQE*, QE-17, 1021(1981).
5. **Private conversation (General Optronics Corp.)**
6. A. Jordan, "Electromagnetic Waves and Radiating Systems"
7. M.P. Jordan, L. Solymar, and P.St.J. Russel, *IEE J. Mic. Opt. Acoust.*, 2, 156(1978).
8. A.H.P.P Leite and O.D.B. Soares, *Proc. S.P.I.E.*, 213, 10(1981).
9. B.R. Brown and A.W. Lohmann, *Appl. Opt.*, 5, 967(1966).
10. A.W. Lohmann and D.P. Paris, *Appl. Opt.*, 6, 1739(1967).
11. A. Nussbaum and R.A. Phillips, "Contemporary Optics for Scientists and Engineers"(Prentice-Hall, Englewood Cliffs, N.J., 1976), pp. 248-270.
12. J.S. Loomis, "Applications of Computer-Generated Holograms in Optical Testing", Ph.D. thesis, Univ. Arizona., (1980).
13. Kodak Minicard II Film, SO-424 product information (1976).